Adsorption of reactive blue 49 onto cross-linked chitosan-based composites containing waste mussel shell and waste active sludge char

Deniz Akin Sahbaz, Sahra Dandil and Caglayan Acikgoz

ABSTRACT

Cross-linked chitosan/waste mussel shell (C/WMS) and chitosan/waste mussel shell/waste active sludge char (C/WMS/WASC) composites were prepared from waste mussel shell, waste active sludge (WAS), and chitosan, and cross-linked with glutaraldehyde. The quantities of chitosan, WMS, and WASC used for the C/WMS and C/WMS/WASC composites were 1:1 and 1:0.5:0.5, respectively. The two adsorbents were characterized for their quality by a scanning electron microscope (SEM), an energy-dispersive X-ray spectroscopy (EDX), and a Brunauer, Emmett and Teller (BET) analyzer. The effects of contact time (0–1,620 mins), pH (1–5), adsorbent dosage (0.01–0.1 g/50 ml), initial dye concentration (20–100 mg/L), and temperature (25–45 °C) on Reactive Blue 49 (RB49) adsorption onto C/WMS and C/WMS/WASC composites were investigated. The maximum RB49 adsorption capacity of C/WMS and C/WMS/WASC composites was 54.7 and 38.8 mg/g, respectively. The experimental data were analyzed by kinetic and isotherm models. The Freundlich isotherm was a good fit for the experimental data of RB49 adsorption on C/WMS and C/WMS/WASC composites, and the adsorption kinetics for both adsorbents were the pseudo-second-order rate equation. All results showed the preparative adsorbents can be used as effective adsorbents for the treatment of waste water contaminated with RB49 since they are low cost and eco-friendly for the environment.

Key words | composite, dye removal, isotherm, kinetic, thermodynamics

HIGHLIGHTS

- Waste active sludge from a membrane bioreactor system and waste mussel shell were evaluated.
- Two new chitosan-based composites were synthesized as eco-friendly adsorbents and used for the removal of Reactive Blue 49.
- Adsorption of Reactive Blue 49 onto the composites followed the Freundlich isotherm model and pseudo-second-order kinetics.
- The composites may be used as alternative adsorbents for wastewater treatment.

Deniz Akin Sahbaz
Department of Chemical Engineering, Faculty of Engineering,
Pamukkale University,
20160 Denizli,
Turkey

Sahra Dandil
Caglayan Acikgoz (corresponding author)
Department of Chemical Engineering, Faculty of Engineering,
Bilecik Seyh Edebali University, Bilecik,
11230 Turkey
E-mail: *caglayan.acikgoz@bilecik.edu.tr*

doi: 10.2166/wst.2021.008

GRAPHICAL ABSTRACT

INTRODUCTION

Synthetic dyes used in various industries like rubber, leather, textile, plastic, paint, paper, cosmetics, etc., for the coloration of products are becoming common water pollutants. These dyes have complex molecular structures and are often highly soluble in water, resistant to aerobic digestion, and quite stable to sunlight and oxidizing agents (Zhao *et al.* 2018). Reactive Blue 49 (RB49) is known as one of the most widely used reactive dyes, which is hazardous and may affect living organisms' life, causing different diseases (Amin Radi *et al.* 2015; Alrobayi *et al.* 2017). Several techniques used in dye removal include coagulation (Morshedi *et al.* 2013), flotation (Liu *et al.* 2010), biological treatment (Khouni *et al.* 2020; Liu *et al.* 2020), reverse osmosis (Nataraj *et al.* 2009), ion exchange (Raghu & Basha 2007), and adsorption (Crini & Badot 2008; Mohammed *et al.* 2020). Among these methods, adsorption is the most promising, easy, and economical method for its high quality of treated effluents and simple design. Many kinds of adsorbents have been reported, such as magnetic iron oxide nanocomposites (Abdullah *et al.* 2019), cellulose-based materials (Putro *et al.* 2019), clay-based minerals (Ngulube *et al.* 2017), agricultural wastes (Dai *et al.* 2018), carbon nanomaterials (Gusain *et al.* 2020), chitosan and its derivatives (Vakili *et al.* 2014). Chitosan-based composites exhibit excellent adsorption performance for dyes because of the large surface area (Zhou *et al.* 2019). Chitosan-based composites have also been proven to be bio-compatible and non-toxic.

Sludge is a byproduct of water discharged from numerous industrial wastewater plants (Hadi *et al.* 2015). Sludge, as a carbon-rich material, is an alternative for the production of activated carbon-based adsorbents. In the past few years, a few studies have focused on the activation and reuse of sludge as a value-added adsorbent for the removal of contaminants from air and water (Rivera-Utrilla *et al.* 2013; Björklund & Li 2017; Akin Sahbaz *et al.* 2019).

Mussel shell is a carbonate-rich waste product of the seafood processing industry. Some factories have developed industrial processes in order to transform shells into rich products. In these processes, shells are washed, crushed, and sieved, and sometimes also calcined (Paradelo *et al.* 2016). In recent years, calcined mussel shells as low cost, easily obtainable, and biodegradable adsorbent materials to treat dyes and heavy metals in wastewater have attracted great interest (Pena-Rodriguez *et al.* 2010; El Haddad *et al.* 2014). However, there is no information currently regarding the use of calcined waste mussel shells (WMS) beside waste active sludge (WAS) as a component of chitosan-based composites, or there is limited information on the removal of RB49 from contaminated solutions using chitosan-based composites, in the literature.

The aim of this study was to prepare the chitosan/waste mussel shell (C/WMS) and chitosan/waste mussel shell/waste active sludge char (C/WMS/WASC) composites as adsorbents for the removal of reactive dyes. The fabricated composites were analyzed using a scanning electron microscope (SEM), Brunauer, Emmett and Teller (BET), and energy-dispersive X-ray spectroscopy (EDX) techniques were subjected for adsorption of RB49 molecules by the batch method. The influence of various adsorption parameters such as contact time, adsorbent dosage, solution pH, initial RB49 concentration, and temperature for the removal of RB49 molecules were determined. The adsorption mechanism, isotherm, kinetic, and thermodynamic parameters were also investigated.

MATERIALS AND METHODS

Materials

Chitosan (with a deacetylation degree of 75–85%) was purchased from Aldrich. The acetic acid (glacial, %100) was used as a solvent to synthesize the composites purchased from Merck. Glutaraldehyde solution (50%) was used as a

crosslinker and supplied by Fluka. WAS was gathered from the membrane bioreactor (MBR) system, containing Trametes Versicolor and used for the decolorization of simulated textile wastewater in the laboratory. WMS was obtained from a seafood processing industry in Bilecik, Turkey. RB49 (purity of 99%) dye used as adsorbate was obtained from a dye factory in Turkey. The pH of the adsorption solutions was adjusted by hydrochloric acid (HCl, Carlo Ebra) and sodium hydroxide (NaOH, Merck) solutions. All chemicals were of analytical grade, without further purification.

Synthesis of the C/WMS and C/WMS/WASC composites

Firstly, WMS was calcinated and WAS were carbonized by chemical activation methods (El Haddad *et al.* 2014; Dandil *et al.* 2019a). After these processes, C/WMS and C/WMS/WASC composites were prepared using the following procedure (Dandil *et al.* 2019b): 1 g of chitosan was dissolved into 75 ml of 5% acetic acid solution under constant stirring in order to get homogeneous mixtures. Certain amounts of WMS and WASC were added in chitosan solutions and the mixtures were stirred with a magnetic stirrer (MR Hei-Standard, Heidolph) overnight, resulting in the formation of the dispersion. The quantities of chitosan, WMS and WASC used for the C/WMS and C/WMS/WASC composites were 1:1 and 1:0.5:0.5, respectively. The C/WMS and C/WMS/WASC mixtures were dripped into alkaline (1 M NaOH) solution with gentle stirring in order to form composite beads. The composite beads were kept in the alkaline mixture for 24 h with continuous stirring. Then, the composite beads were removed from the alkaline solution and washed with distilled water many times to attain a neutral pH. Subsequently, the composites were shaken in glutaraldehyde solution (2.5 w %) for 15 h at 60 °C. After the cross-linking reaction, the composites were washed using distilled water to remove free glutaraldehyde and left to dry at room temperature. Finally, they were placed in a glass bottle and stored in a desiccator until further use in adsorption studies.

Characterization of the C/WMS and C/WMS/WASC composites

The surface morphology of the C/WMS and C/WMS/WASC composites was investigated with an SEM (Leo 1430 VP, Zeiss). To analyze the composition of the composites, elementary characterization was carried out using an EDX (Leo 1430 VP, Zeiss) analyzer. Surface areas of the composites were measured by a BET (ASAP 2020, Micromeritics) instrument using the nitrogen intrusion technique. The microstructures of the composites were characterized using physical adsorption/desorption of nitrogen at 77 K.

Batch adsorption studies

Batch adsorption tests were performed on a certain amount of C/WMS and C/WMS/WASC composites using 50 mL of the RB49 dye solutions of known concentration. The effect of pH on RB49 adsorption was investigated in the pH ranges between 1 and 5. To optimize the adsorbent dosage for the adsorption capacity and removal of RB49 dye from aqueous solution, the adsorbent dosage was varied from 0.01 to 0.1 g/50 mL for C/WMS and C/WMS/WASC composites. Initial concentrations of RB49 dye solutions in the range of 20 mg/L to 100 mg/L were investigated. Finally, the adsorption experiments were carried out at 25, 35, and 45 °C to determine the effect of temperature on the adsorption process and the thermodynamic parameters of the process. In adsorption processes, the dye solutions were agitated in a thermostat shaker (H11960, Termal) at 150 rpm until adsorption reached equilibrium. Afterward, the suspension of the adsorbent was centrifuged in order to obtain the supernatant. The concentration of dye ions remaining in the supernatant solutions was analyzed spectrophotometrically at 586 nm wavelength using a UV–vis spectrophotometer (Cary 60 UV-Vis, Agilent). All experiments were performed in triplicate.

The adsorption capacity (q_e) and the dye removal percentage (R %) were calculated according to the following equations:

$$q_e = \frac{(C_0 - C_e)V}{m} \quad (1)$$

$$Removal\ (\%) = \frac{(C_0 - C_e)}{C_0} \times 100 \quad (2)$$

where C_0 and C_e (mg/L) are the initial and equilibrium RB49 dye concentrations in the liquid phase, respectively. V (L) is the volume of solution, and m (g) is the amount of adsorbent.

RESULTS AND DISCUSSION

Characterization of C/WMS and C/WMS/WASC composites

The morphology and surface variations of the C/WMS and C/WMS/WASC composites were investigated at different

magnifications (125 ×, 500 ×, and 3000 ×) using SEM analysis and micrographs as shown in Figure 1. The microscopic observations showed that both C/WMS and C/WMS/WASC composites have spherical shapes and porous structures.

The EDX analyses of C/WMS and C/WMS/WASC composites were employed to depict the elemental composition of the composites. As can be seen in Figure 2, carbon (C), oxygen (O), calcium (Ca), and chlorine (Cl) elements were detected in all composites, whereas silicon (Si), phosphorus

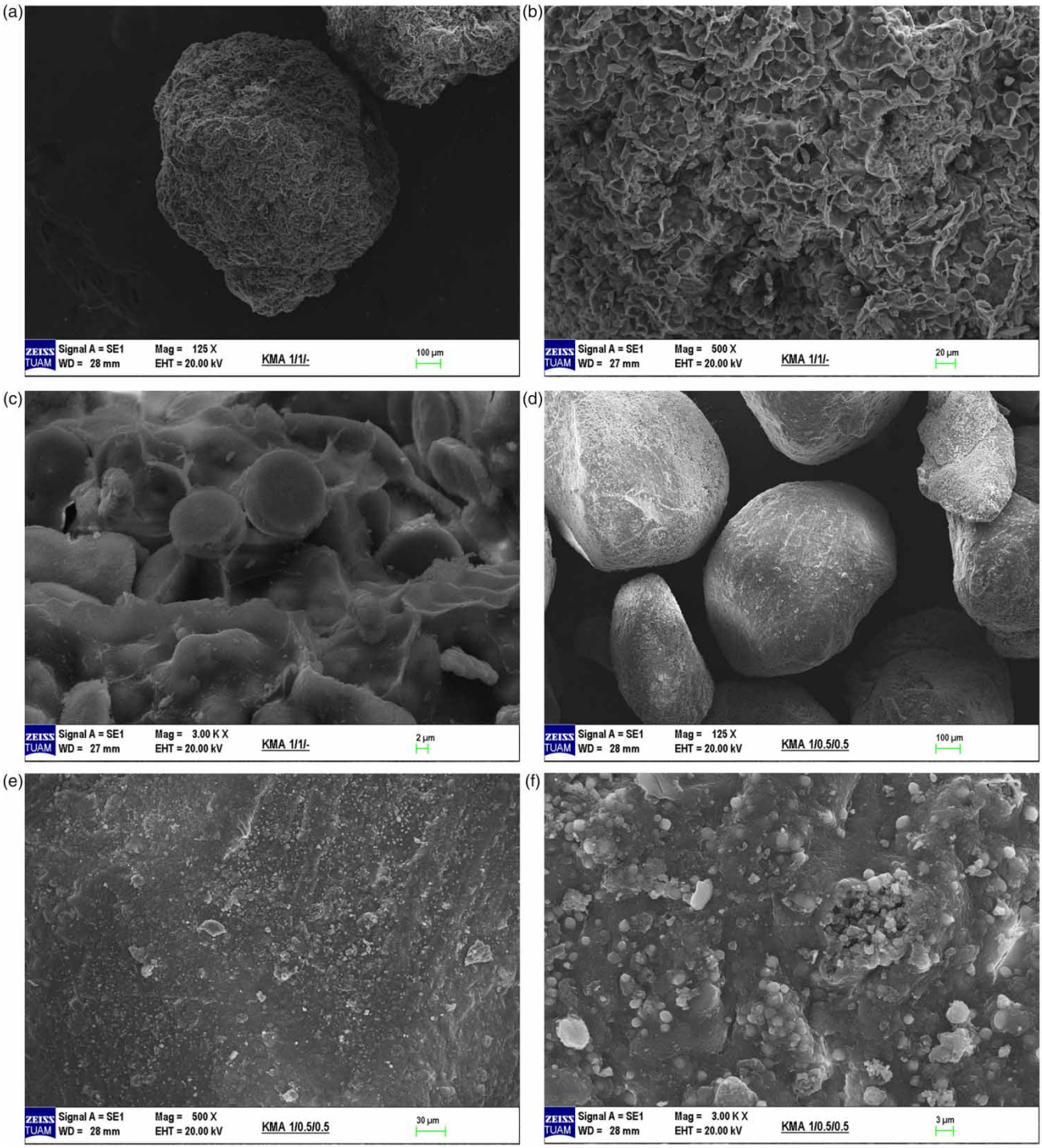

Figure 1 | SEM images of the C/WMS (a, b, c) and C/WMS/WASC composites (d, e, f).

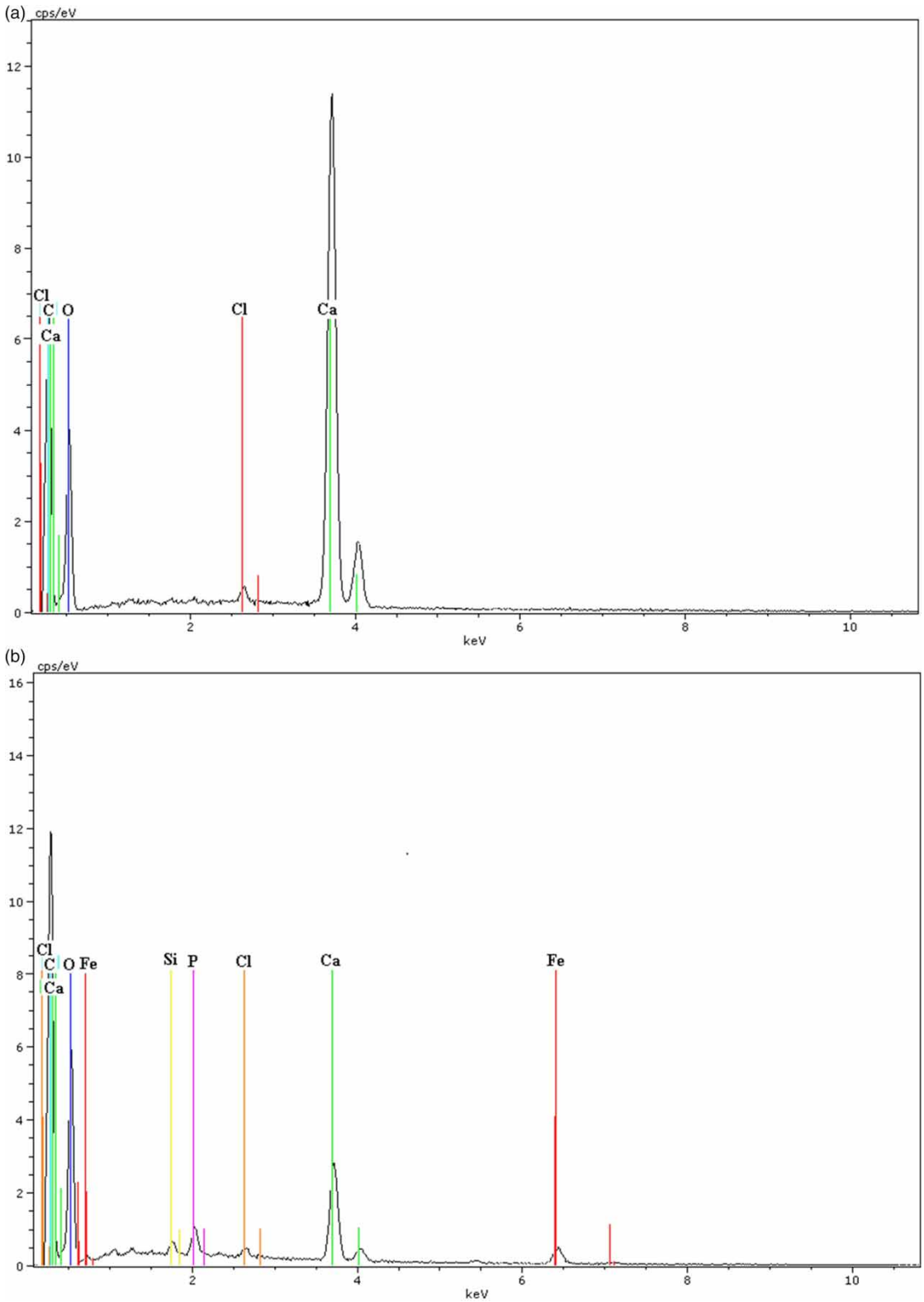

Figure 2 | EDX patterns of the C/WMS (a) and C/WMS/WASC composites (b).

(P), and iron (Fe) elements were only detected in the C/WMS/WASC composites due to the waste active sludge char content of the composites. The waste active sludge contains a trace amount of inorganic compound due to the biological treatment of textile wastewater in the MBR system.

The quantitative analysis of the composites is given in Table 1. The mass fraction of Ca, C and O are 22.30%, 25.61%, 51.67% and 9.38%, 35.96%, 54.46% for the C/WMS and C/WMS/WASC composites, respectively.

In the adsorption process, the surface area of the adsorbents is the most important factor. When the surface area is high, there will be more active surface sites for adsorption of the dye molecules. In the BET analysis, the surface areas of the C/WMS and C/WMS/WASC composites were determined as 15.0 m^2/g and 7.6 m^2/g, respectively. The higher adsorption capacity of C/WMS than that of C/WMS/WASC composites could be linked to the higher BET value resulting in more availability of active adsorption sites (Kanakaraju *et al.* 2020).

Effect of contact time

Figure 3 presents the RB49 adsorption by C/WMS and C/WMS/WASC composites as a function of contact time at different solution pH. The RB49 dye adsorption capacities of C/WMS and C/WMS/WASC composites increase by time up to the adsorption equilibrium. While the adsorption of dye is quite rapid initially, the rate of adsorption becomes slower with time and reaches a constant value at equilibrium. The equilibrium time is 1,620 min for both C/WMS and C/WMS/WASC composites. The results indicate that the C/WMS and C/WMS/WASC composites have nearly the same adsorption rates for RB49 dye. The rapid uptake at the beginning of the adsorption processes could be better explained by the high affinity of C/WMS and C/WMS/WASC composites towards RB49 dye molecules. Moreover, this adsorption behavior could be due to the adsorption of RB49 dye onto the external surface C/WMS and C/WMS/WASC composites and the availability of a large excess of adsorption binding sites. The following slow adsorption behavior is attributed to the penetration-diffusion of RB49 molecules into the inner surface of C/WMS and C/WMS/WASC composites (Hsini *et al.* 2020a).

Table 1 | Quantitative results of EDS analysis

	C/WMS composites		C/WMS/WASC composites	
Elements	**Mass %**	**Atomic %**	**Mass %**	**Atomic %**
Carbon (C)	25.61	35.96	35.32	44.62
Oxygen (O)	51.67	54.46	54.25	51.44
Chlorine (Cl)	0.42	0.20	0.48	0.20
Calcium (Ca)	22.30	9.38	5.42	2.05
Silicon (Si)	–	–	0.70	0.38
Phosphorus (P)	–	–	1.20	0.59
Iron (Fe)	–	–	2.64	0.72

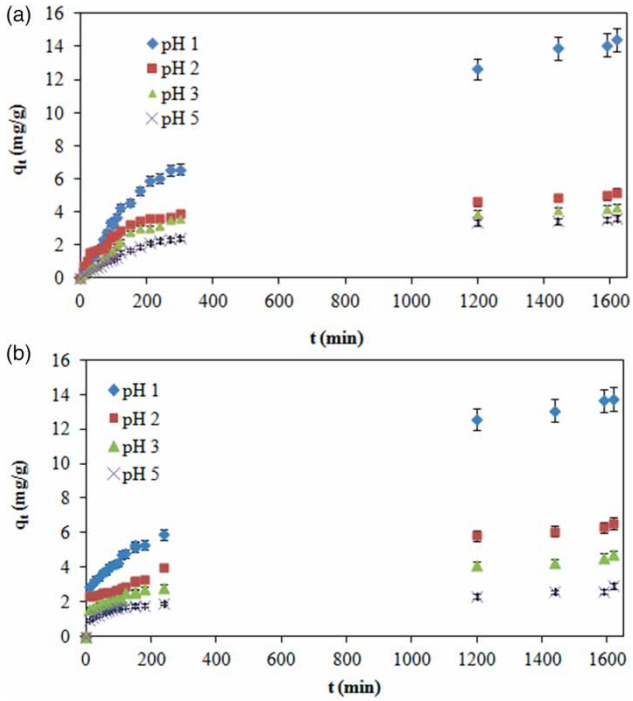

Figure 3 | Effect of contact time on the RB49 adsorption onto the C/WMS (a) and C/WMS/WASC (b) composites at different solution pH (adsorbent dosage: 0.1 g/50 ml; 25 °C; 150 rpm; pH 1–5; initial RB49 concentration: 60 mg/L).

Adsorption kinetics

Two widely used kinetic models, pseudo-first-order and pseudo-second-order kinetic models, were applied to the experimental data in order to investigate the adsorption dynamics of RB49 on the C/WMS and C/WMS/WASC composites, as well as the mechanisms involved in the adsorption system.

The pseudo-first-order model is expressed by the following linearized form (Lagergren 1898):

$$\log(q_e - q_t) = \log q_e - \frac{k_1}{2.303}t \quad (3)$$

The linearized form of the pseudo-second-order model proposed by Ho & McKay (1999) is expressed as follows:

$$\frac{t}{q_t} = \frac{1}{k_2 q_e^2} + \frac{1}{q_e}t \quad (4)$$

where q_e and q_t are the amounts of RB49 adsorbed (mg/g) on the adsorbent at equilibrium and at time t (min), respectively. k_1 is the rate constant of the pseudo-first-order model (1/min), and k_2 is the pseudo-second-order rate constant (g/(mg min)). The values of q_e and k_1 can be calculated from the intercept and slope of the linear plot of $\log(q_e - q_t)$ versus t (Figure 4), and k_2 can be determined experimentally from the slope and intercept of the plot of t/q_t versus t (Figure 5).

The results of the kinetic parameters for RB49 adsorption of C/WMS and C/WMS/WASC composites as calculated from the linear plots of the two kinetic models are presented in Table 2. The pseudo-second-order kinetic model fitted the experimental data of both C/WMS and C/WMS/WASC composites better than the pseudo-first-order model, resulting in high correlation coefficients. Additionally, the theoretical q_e ($q_{e,\mathrm{cal}}$) values of C/WMS and C/WMS/WASC composites were both very close to experimental q_e ($q_{e,\mathrm{exp}}$) values, indicating that the adsorption process followed the pseudo-second-order kinetic model and the RB49 dye adsorption of C/WMS and C/WMS/WASC composites was dominated by a chemical process.

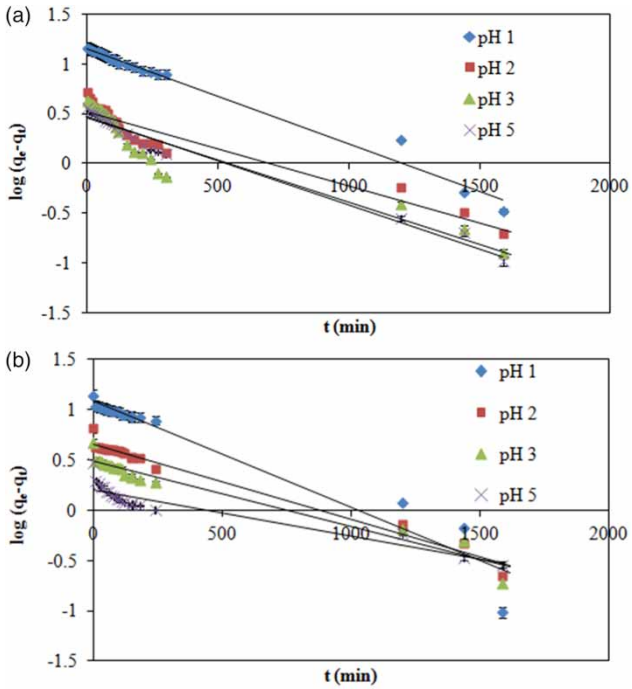

Figure 4 | Pseudo first order kinetic plots for the adsorption of RB49 dye on the C/WMS (a) and C/WMS/WASC (b) composites (adsorbent dosage: 0.1 g/50 ml; 25 °C; 150 rpm; pH 1–5; initial RB49 concentration: 60 mg/L).

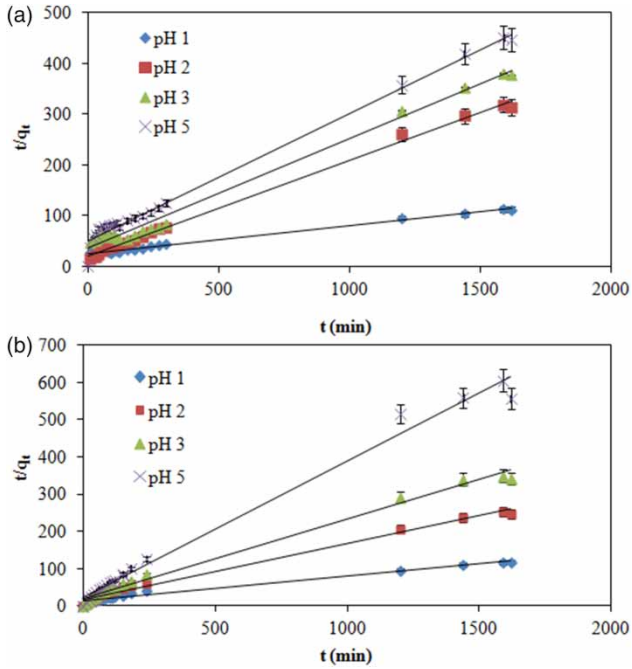

Figure 5 | Pseudo second order kinetic plots for the adsorption of RB49 dye on the C/WMS (a) and C/WMS/WASC (b) composites (adsorbent dosage: 0.1 g/50 ml; 25 °C; 150 rpm; pH 1–5; initial RB49 concentration: 60 mg/L).

Effect of adsorbent dosage

To optimize the adsorbent dosage for the adsorption capacities of C/WMS and C/WMS/WASC composites and the percentages of RB49 removal from aqueous solution, the effect of the adsorbent dosage was investigated and shown in Figure 6.

The percentage of dye adsorption increased from 18.2 to 48.0% and from 12.9 to 45.8%, by increasing the adsorbent mass from 0.01/50 mL to 0.1 g/50 mL for C/WMS and C/WMS/WASC composites, respectively. This increase may be due to the number of adsorption sites increased with the number of adsorbents. The adsorption capacities decreased from 54.7 mg/g to 14.4 mg/g and from 38.8 mg/g to 13.7 mg/g by increasing the adsorbent mass from 0.01/50 mL to 0.1 g/50 mL for C/WMS and C/WMS/WASC composites, respectively.

The adsorption capacity of C/WMS and C/WMS/WASC composites for reactive blue dye ions are substantially high compared to other adsorbents, as seen in Table 3.

Equilibrium isotherms

The two most common isotherm models, Langmuir and Freundlich, were applied to the experimental data. Freundlich and Langmuir equations are written as (Freundlich

Table 2 | Kinetic parameters of the adsorption of RB49 onto the C/WMS and C/WMS/WASC composites in aqueous solution

			Lagergren first order kinetic model			Pseudo-second order kinetic model		
Adsorbent	**pH**	$q_{e,exp}$ (mg/g)	$q_{e,cal}$ (mg/g)	k_1 (min^{-1})	R^2	$q_{e,cal}$ (mg/g)	$k_2 \times 10^3$ ($g \cdot mg^{-1} \cdot min^{-1}$)	R^2
C/WMS	1	14.41	14.13	0.0023	0.9820	18.31	0.1155	0.9947
	2	5.18	3.29	0.0016	0.9099	5.29	1.7947	0.9972
	3	4.30	2.91	0.0018	0.8558	4.66	1.2465	0.9905
	5	3.63	2.94	0.0020	0.9719	3.98	1.2369	0.9900
C/WMS/WASC	1	13.73	12.08	0.0023	0.9394	14.88	0.3527	0.9744
	2	6.54	4.53	0.0016	0.9748	6.66	1.3775	0.9899
	3	4.75	3.07	0.0014	0.9433	4.70	2.3696	0.9915
	5	2.92	1.60	0.0011	0.8725	2.74	6.0771	0.9907

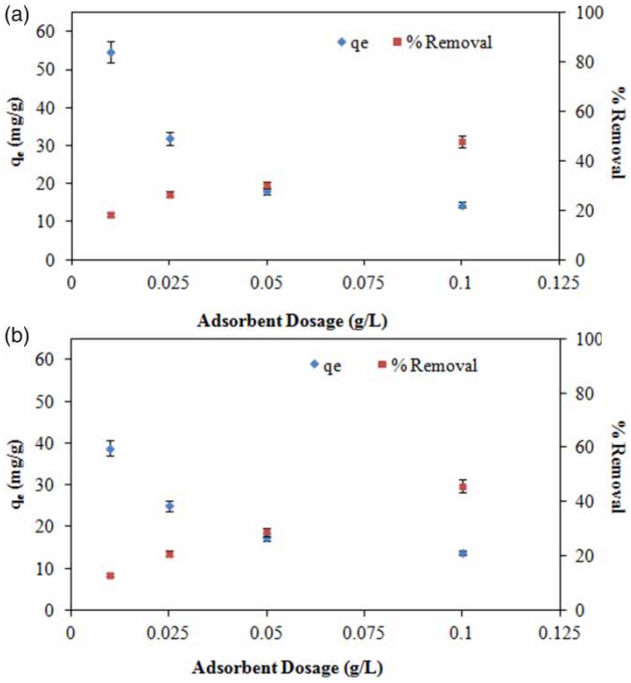

Figure 6 | Effect of adsorbent dosage on the RB49 removal % and adsorption capacities for (a) the C/WMS and (b) C/WMS/WASC composites (adsorbent dosage: 0.01–0.1 g/50 ml; 25 °C; 150 rpm; pH 1; initial RB49 concentration: 60 mg/L).

Table 3 | Comparison of the adsorption capacities of various adsorbents for Reactive Blue dye ions

Adsorbent	**Dye**	q_{max} (mg/g)	**References**
Citrus sinensis biosorbent	RB49	27.41	Asgher & Bhatti (2012)
Acetic acid treated *Citrus* waste biomass	RB49 Reactive Blue 19	33.53 23.31	Asgher & Bhatti (2012)
Capsicum annuum seeds (acetone treated)	RB49	96.35	Akar *et al.* (2011)
Natural wheat straw	Reactive Blue	1.63	Mousa & Taha (2015)
Modified wheat straw	Reactive Blue	11.79	Mousa & Taha (2015)
Modified silk cotton hull waste	Reactive Blue MR	13.54	Thangamani *et al.* (2007)
Chitosan-activated sludge composites	RB49	16.91	Akin Sahbaz *et al.* (2019)
C/WMS/WASC composites	RB49	38.8	Present study
C/WMS composites	RB49	54.7	Present study

1906; Langmuir 1918; Freundlich & Heller 1939):

$$\ln q_e = \left(\frac{1}{n}\right) \ln C_e + \ln K_F \tag{5}$$

$$\frac{C_e}{q_e} = \frac{C_e}{q_{\max}} + \frac{1}{q_{\max} K_L} \tag{6}$$

where q_e (mg/g) and C_e (mg/L) are the equilibrium adsorption capacity and the equilibrium dye concentration in solution. K_F is the Freundlich constant, and n is the heterogeneity factor indicating the intensity of adsorption. $q_{\max}$ (mg/g) is the theoretical maximum adsorption capacity of absorbents, and K_L (L/mg) is the Langmuir adsorption constant. Figure 7 shows the plots of the Freundlich and Langmuir adsorption isotherm models.

Table 4 shows the Freundlich and Langmuir isotherm constants. The comparison of the correlation coefficient (R^2) values shows that the Freundlich isotherm model yields a better fit to the experimental data of the adsorption behavior of C/WMS and C/WMS/WASC composites than the Langmuir isotherm model. The Freundlich model is based on the assumption that adsorption occurs on multilayer and heterogeneous surfaces of the adsorbent due to

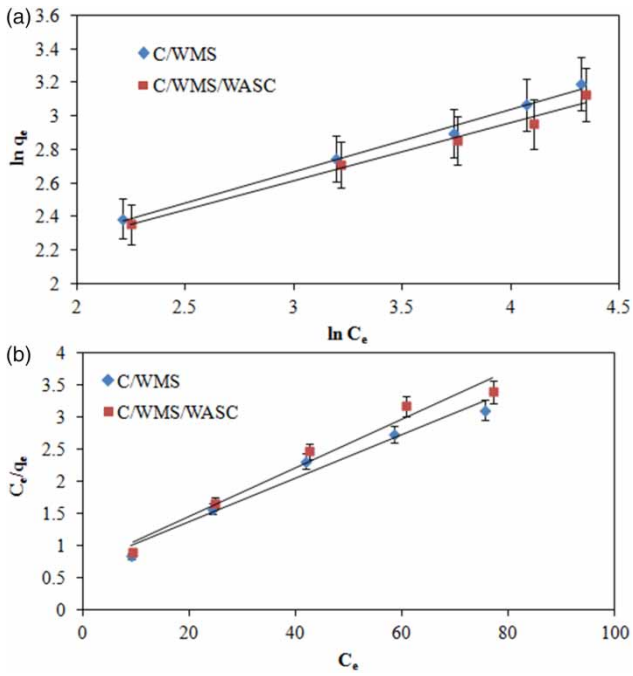

Figure 7 | Linear forms of the adsorption isotherms: (a) Freundlich model and (b) Langmuir model (adsorbent dosage: 0.05 g/50 ml; 25 °C; 150 rpm; pH 1; initial RB49 concentration: 20–100 mg/L).

Table 4 | Parameters for Freundlich and Langmuir isotherm models for the adsorption of RB49 onto the C/WMS and C/WMS/WASC composites

		Adsorbent	
Isotherms	**Parameters**	**C/WMS**	**C/WMS/WASC**
Freundlich	K_F [mg/g (L/g)$^{1/n}$]	4.7176	4.8148
	n	2.6867	2.8802
	R^2	0.9919	0.9856
Langmuir	q_m (mg/g)	29.50	26.45
	K_L (L/mg)	0.0492	0.0547
	R^2	0.9714	0.9698

the diversity of adsorption sites (Crini & Badot 2008). Moreover, as shown in Table 4, the values of n are greater than 1, confirming that the adsorption processes are favorable. The lower values of both K_F and n for C/WMS composites compared with C/WMS/WASC composites reflect the lower affinity of RB49 for adsorption surfaces (Hua *et al.* 2018).

Adsorption thermodynamics

The thermodynamic parameters including the Gibbs free energy (ΔG^o), enthalpy change (ΔH^o), and entropy change (ΔS^o) for the adsorption of the RB49 dye on the C/WMS and C/WMS/WASC composites were determined using the Van't Hoff equation:

$$\ln\left(\frac{q_e}{C_e}\right) = \frac{\Delta S^\circ}{R} - \frac{\Delta H^\circ}{RT} \quad (7)$$

where R (8.314 J K^{-1} mol^{-1}) and T (K) are the universal gas constant and the absolute temperature, respectively. By using the plot of the Van't Hoff equation as ln (q_e/C_e) against 1/T (Figure 8), ΔS° and ΔH° can be estimated by the slope and intercept, respectively.

Table 5 indicates the determined values of thermodynamic parameters for RB49 dye adsorption. A decrease in randomness is indicated by negative values of entropy change whereas the exothermic nature of the process is indicated by the negative values of enthalpy. Positive ΔG° values indicate that the adsorption process is non-spontaneous in the temperature range of 298–318 K (Asgher & Bhatti 2012). Furthermore, the increasing pattern of ΔG° magnitudes upon rising the temperature further suggests that the RB49 molecules adsorption becomes more feasible at lower temperatures (Hsini *et al.* 2020b).

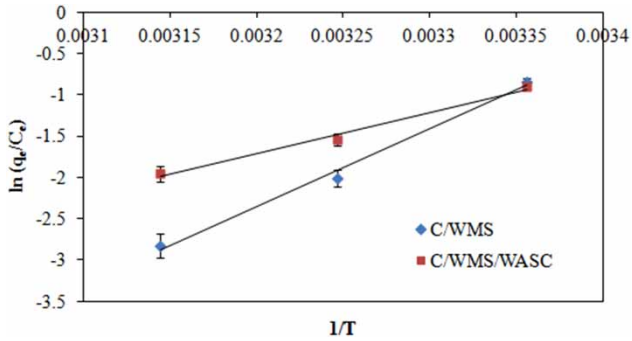

Figure 8 | Plot of ln K_L versus 1/T for the estimation of thermodynamic parameters.

Table 5 | Thermodynamic parameters for the adsorption of RB49 onto the C/WMS and C/WMS/WASC composites

Adsorbent	**Temperature (K)**	**ΔG° (kJ mol^{-1})**	**ΔH° (kJ mol^{-1})**	**ΔS° (kJ mol^{-1} K^{-1})**
C/WMS	298	2.198	− 78.54	− 0.2709
	308	4.907		
	318	7.616		
C/WMS/WASC	298	2.313	− 41.72	− 0.1478
	308	3.790		
	318	5.268		

CONCLUSION

The present study demonstrates that the chitosan-based composites containing WMS and WASC can be used as an effective alternative and low-cost adsorbent for the treatment of water/wastewater contaminated with RB49 dye. It has been observed that the two adsorbents have high resistance to acidic conditions and are very effective in removing the organic pollutants in an acidic environment.

Approximately 48.0% and 45.8% RB49 dyes were removed from the aqueous solution using the C/WMS and C/WMS/WASC composites in 1,620 minutes, respectively.

The maximum RB49 adsorption capacity of C/WMS and C/WMS/WASC composites were 54.7 and 38.8 mg/g, respectively. The pseudo-second order kinetic model and the Freundlich isotherm model were successfully fitted to describe the adsorption mechanism for both composites.

Thermodynamic parameters for the adsorption of RB49 onto the C/WMS and C/WMS/WASC composites like ΔG°(298 K), ΔH°, and ΔS° changes have been calculated as (2.198 kJ·mol^{-1}) and (2.313 kJ·mol^{-1}); (−78.54 kJ·mol^{-1}) and (−41.72 kJ·mol^{-1}); (−0.2709 kJ·mol^{-1}·K^{-1}) and (−0.1478 kJ·mol^{-1}·K^{-1}), respectively.

All in all, the C/WMS and C/WMS/WASC composites are quite promising adsorbents and may be used as alternative approaches for RB49 dye removal from contaminated water.

DATA AVAILABILITY STATEMENT

All relevant data are included in the paper or its Supplementary Information.

REFERENCES

Abdullah, N. H., Shameli, K., Abdullah, E. C. & Abdullah, L. C. 2019 Solid matrices for fabrication of magnetic iron oxide nanocomposites: synthesis, properties, and application for the adsorption of heavy metal ions and dyes. *Composites Part B: Engineering* **162**, 538–568. doi: 10.1016/j.compositesb.2018.12.075.

Akar, S. T., Gorgulu, A., Akar, T. & Celik, S. 2011 Decolorization of Reactive Blue 49 contaminated solutions by capsicum annuum seeds: batch and continuous mode biosorption applications. *Chemical Engineering Journal* **168** (1), 125–133. doi: 10.1016/j.cej.2010.12.049.

Akin Sahbaz, D., Dandil, S. & Acikgoz, C. 2019 Kinetic studies on the removal of Reactive Blue 49 dye from aqueous solution onto chitosan-activated sludge composite particles. *Biological and Chemical Research* **6**, 19–29.

Alrobayi, E. M., Algubili, A. M., Aljeboree, A. M., Alkaim, A. F. & Hussein, F. H. 2017 Investigation of photocatalytic removal and photonic efficiency of maxilon blue dye GRL in the presence of TiO_2 nanoparticles. *Particulate Science and Technology* **35** (1), 4–20. doi: 10.1080/02726351.2015.1120836.

Amin Radi, M., Nasirizadeh, N., Rohani-Moghadam, M. & Dehghani, M. 2015 The comparison of sonochemistry, electrochemistry and sonoelectrochemistry techniques on decolorization of CI Reactive Blue 49. *Ultrasonics Sonochemistry* **27**, 609–615. doi: 10.1016/j.ultsonch.2015.04.021.

Asgher, M. & Bhatti, H. N. 2012 Evaluation of thermodynamics and effect of chemical treatments on sorption potential of Citrus waste biomass for removal of anionic dyes from aqueous solutions. *Ecological Engineering* **38**, 79–85. doi: 10.1016/j.ecoleng.2011.10.004.

Björklund, K. & Li, L. Y. 2017 Adsorption of organic stormwater pollutants onto activated carbon from sewage sludge. *Journal of Environmental Management* **197**, 490–497. doi: 10.1016/j.jenvman.2017.04.011.

Crini, G. & Badot, P. M. 2008 Application of chitosan, a natural aminopolysaccharide, for dye removal from aqueous solutions by adsorption processes using batch studies: a review of recent literature. *Progress in Polymer Science* **33** (4), 399–447. doi: 10.1016/j.progpolymsci.2007.11.001.

Dai, Y., Sun, Q., Wang, W., Lu, L., Liu, M., Li, J., Yang, S., Sun, Y., Zhang, K., Xu, J., Zheng, W., Hu, Z., Yang, Y., Gao, Y., Chen, Y., Zhang, X., Gao, F. & Zhang, Y. 2018 Utilizations of agricultural waste as adsorbent for the removal of contaminants: a review. *Chemosphere* **211**, 235–253. doi: 10.1016/j.chemosphere.2018.06.179.

Dandil, S., Akin Sahbaz, D. & Acikgoz, C. 2019a High performance adsorption of hazardous triphenylmethane dye-crystal violet onto calcinated waste mussel shells. *Water Quality Research Journal Canada* **54** (3), 249–256. doi: 10.2166/wqrj.2019.050.

Dandil, S., Akin Sahbaz, D. & Acikgoz, C. 2019b Adsorption of Cu (II) ions onto crosslinked chitosan/waste active sludge char (WASC) beads: kinetic, equilibrium, and thermodynamic study. *International Journal of Biological Macromolecules* **136**, 668–675. doi: 10.1016/j.ijbiomac.2019.06.063.

El Haddad, M., Regti, A., Slimani, R. & Lazar, S. 2014 Assessment of the biosorption kinetic and thermodynamic for the removal of safranin dye from aqueous solutions using calcined mussel shells. *Journal of Industrial and Engineering Chemistry* **20** (2), 717–724. doi: 10.1016/j.jiec.2013.05.038.

Freundlich, H. M. F. 1906 Over the adsorption in solution. *The Journal of Physical Chemistry* **57**, 385–471.

Freundlich, H. & Heller, W. 1939 The adsorption of cis-and trans-azobenzene. *Journal of the American Chemical Society* **61** (8), 2228–2230.

Gusain, R., Kumar, N. & Ray, S. S. 2020 Recent advances in carbon nanomaterial-based adsorbents for water purification.

Coordination Chemistry Reviews **405**, 213111. https://doi.org/10.1016/j.ccr.2019.213111.

Hadi, P., Xu, M., Ning, C., Lin, C. S. K. & McKay, G. 2015 A critical review on preparation, characterization and utilization of sludge-derived activated carbons for wastewater treatment. *Chemical Engineering Journal* **260**, 895–906. doi: 10.1016/j.cej.2014.08.088.

Ho, Y. S. & McKay, G. 1999 Pseudo-second order model for sorption processes. *Process Biochemistry* **34**, 451–465. doi: 10.1016/S0032-9592(98)00112-5.

Hsini, A., Essekri, A., Aarab, N., Laabd, M., Addi, A. A., Lakhmiri, R. & Albourine, A. 2020a Elaboration of novel polyaniline@Almond shell biocomposite for effective removal of hexavalent chromium ions and Orange G dye from aqueous solutions. *Environmental Science and Pollution Research* **27**, 15245–15258. doi: 10.1007/s11356-020-08039-1.

Hsini, A., Naciri, Y., Laabd, M., El Ouardi, M., Ajmal, Z., Lakhmiri, R., Boukherroub, R. & Albourine, A. 2020b Synthesis and characterization of arginine-doped polyaniline/walnut shell hybrid composite with superior clean-up ability for chromium (VI) from aqueous media: equilibrium, reusability and process optimization. *Journal of Molecular Liquids* **316**, 113832. doi: 10.1016/j.molliq.2020.113832.

Hua, T., Haynes, R. J. & Zhou, Y. F. 2018 Competitive adsorption and desorption of arsenate, vanadate, and molybdate onto the low-cost adsorbent materials alum water treatment sludge and bauxite. *Environmental Science and Pollution Research* **25**, 34053–34062. doi: 10.1007/s11356-018-3301-7.

Kanakaraju, D., bin Ya, M. H., Lim, Y. C. & Pace, A. 2020 Combined adsorption/photocatalytic dye removal by copper-titania-fly ash composite. *Surfaces and Interfaces* **19**, 100534. doi: 10.1016/j.surfin.2020.100534.

Khouni, I., Louhichi, G. & Ghrabi, A. 2020 Assessing the performances of an aerobic membrane bioreactor for textile wastewater treatment: influence of dye mass loading rate and biomass concentration. *Process Safety and Environmental Protection* **135**, 364–382. doi: 10.1016/j.psep.2020.01.011.

Lagergren, S. 1898 Zur theorie Der Sogenannten adsorption geloster stoffe Kungliga Svenska Vetenskapsakademiens. *Handlingar* **24**, 1–39.

Langmuir, I. 1918 The adsorption of gases on plane surfaces of glass, mica and platinum. *Journal of the American Chemical Society* **40**, 1361–1403.

Liu, Y., Li, K., Xu, W., Du, B., Wei, Q., Liu, B. & Wei, D. 2020 GO/PEDOT: NaPSS modified cathode as heterogeneous electro-Fenton pretreatment and subsequently aerobic granular sludge biological degradation for dye wastewater treatment. *Science of The Total Environment* **700**, 134536. doi: 10.1016/j.scitotenv.2019.134536.

Liu, S., Wang, Q., Ma, H., Huang, P., Li, J. & Kikuchi, T. 2010 Effect of micro-bubbles on coagulation flotation process of dyeing wastewater. *Separation and Purification Technology* **71**, 337–346. doi: 10.1016/j.seppur.2009.12.021.

Mohammed, B. B., Hsini, A., Abdellaoui, Y., Abou Oualid, H., Laabd, M., El Ouardi, M., Ait Addi, A., Yamni, K. & Tijani, N. 2020 Fe-ZSM-5 zeolite for efficient removal of basic Fuchsin dye from aqueous solutions: synthesis, characterization and adsorption process optimization using BBD-RSM modeling. *Journal of Environmental Chemical Engineering* **8**, 104419.

Morshedi, D., Mohammadi, Z., Boojar, M. M. A. & Aliakbari, F. 2013 Using protein nanofibrils to remove azo dyes from aqueous solution by the coagulation process. *Colloids and Surfaces B: Biointerfaces* **112**, 245–254. doi: 10.1016/j.colsurfb.2013.08.004.

Mousa, K. M. & Taha, A. H. 2015 Adsorption of Reactive Blue dye onto natural and modified wheat straw. *Journal of Chemical Engineering & Process Technology* **6** (6), 1–6. doi: 10.4172/2157-7048.1000260.

Nataraj, S. K., Hosamani, K. M. & Aminabhavi, T. M. 2009 Nanofiltration and reverse osmosis thin film composite membrane module for the removal of dye and salts from the simulated mixtures. *Desalination* **249**, 12–17. doi: 10.1016/j.desal.2009.06.008.

Ngulube, T., Gumbo, J. R., Masindi, V. & Maity, A. 2017 An update on synthetic dyes adsorption onto clay based minerals: a state-of-art review. *Journal of Environmental Management* **191**, 35–57. doi: 10.1016/j.jenvman.2016.12.031.

Paradelo, R., Conde-Cid, M., Cutillas-Barreiro, L., Arias-Estevez, M., Novoa-Munoz, J. C., Álvarez-Rodriguez, E., Fernandez-Sanjurjo, M. J. & Nunez-Delgado, A. 2016 Phosphorus removal from wastewater using mussel shell: investigation on retention mechanisms. *Ecological Engineering* **97**, 558–566. doi: 10.1016/j.ecoleng.2016.10.066.

Pena-Rodriguez, S., Fernandez-Calvino, D., Novoa-Munoz, J. C., Arias-Estevez, M., Nunez-Delgado, A., Fernandez-Sanjurjo, M. J. & Alvarez-Rodriguez, E. 2010 Kinetics of Hg (II) adsorption and desorption in calcined mussel shells. *Journal of Hazardous Materials* **180** (1–3), 622–627. doi: 10.1016/j.jhazmat.2010.04.079.

Putro, J. N., Santoso, S. P., Soetaredjo, F. E., Ismadji, S. & Ju, Y. H. 2019 Nanocrystalline cellulose from waste paper: adsorbent for azo dyes removal. *Environmental Nanotechnology, Monitoring & Management* **12**, 100260. doi: 10.1016/j.enmm.2019.100260.

Raghu, S. & Basha, C. A. 2007 Chemical or electrochemical techniques, followed by ion exchange, for recycle of textile dye wastewater. *Journal of Hazardous Materials* **149** (2), 324–330. doi: 10.1016/j.jhazmat.2007.03.087.

Rivera-Utrilla, J., Gomez-Pacheco, C. V., Sanchez-Polo, M., Lopez-Penalver, J. J. & Ocampo-Perez, R. 2013 Tetracycline removal from water by adsorption/bioadsorption on activated carbons and sludge-derived adsorbents. *Journal of Environmental Management* **131**, 16–24. doi: 10.1016/j.jenvman.2013.09.024.

Thangamani, K. S., Sathishkumar, M., Sameena, Y., Vennilamani, N., Kadirvelu, K., Pattabhi, S. & Yun, S. E. 2007 Utilization of modified silk cotton hull waste as an adsorbent for the removal of textile dye (reactive blue MR) from aqueous solution. *Bioresource Technology* **98** (6), 1265–1269. doi: 10.1016/j.biortech.2006.05.010.

Vakili, M., Rafatullah, M., Salamatinia, B., Abdullah, A. Z., Ibrahim, M. H., Tan, K. B., Gholami, Z. & Amouzgar, P. 2014 Application of chitosan and its derivatives as adsorbents for

dye removal from water and wastewater: a review. *Carbohydrate Polymers* **113**, 115–130. doi: 10.1016/j.carbpol.2014.07.007.

Zhao, J., Zou, Z., Ren, R., Sui, X., Mao, Z., Xu, H., Zhong, Y., Zhang, L. & Wang, B. 2018 Chitosan adsorbent reinforced with citric acid modified β-cyclodextrin for highly efficient removal of dyes from reactive dyeing effluents. *European Polymer Journal* **108**, 212–218. doi: 10.1016/j.eurpolymj.2018.08.044.

Zhou, Y., Lu, J., Zhou, Y. & Liu, Y. 2019 Recent advances for dyes removal using novel adsorbents: a review. *Environmental Pollution* **252**, 352–365. doi: 10.1016/j.envpol.2019.05.072.

First received 3 November 2020; accepted in revised form 19 December 2020. Available online 2 January 2021